ECOHYDROLOGY
Ecohydrol. (2010)
Published online in Wiley InterScience
(www.interscience.wiley.com) DOI: 10.1002/eco.149

Surface and groundwater dynamics in the sedimentary plains of the Western Pampas (Argentina)

R. Aragón,[1,2] E. G. Jobbágy[1]* and E. F. Viglizzo[3]

[1] *Grupo de Estudios Ambientales, IMASL, Universidad Nacional de San Luis/CONICET. Ejercito de los Andes 950 (5700) San Luis, Argentina*
[2] *Instituto de Ecología Regional (IER), Facultad de Ciencias Naturales, Universidad Nacional de Tucumán & CONICET—CC 34 (4107) Tucumán, Argentina*
[3] *INTA EEA Anguil & INCITAP-CONICET, Anguil RN 5 km 580 (6326) La Pampa, Argentina*

ABSTRACT

Sedimentary plains with extremely flat topography, such as the Pampas in Argentina, often display flooding–drought cycles. Changes in water table depth and surface water coverage affect natural and cultivated vegetation, wildlife, and people. Here, we describe groundwater dynamics and water-body expansion in a 10-year flooding cycle in the valuable agricultural lands of Western Pampas. We analysed water-table depth, surface water coverage, and rainfall from 1996 to 2005 covering ~28 000 km^2. We characterized the dynamics of water storage based on groundwater observations and remote sensing estimates of the coverage (LANDSAT) and elevation (ENVISAT) of water bodies as well as water storage anomalies captured by the gravity recovery and climate experiment (GRACE). Surface water coverage fluctuated from 3 to 28% and groundwater levels displayed a ~2·5 m change. Regional water storage raised by ~800 mm with 63% of this water accretion accounted by groundwater. Ground and surface water dynamics were closely coupled but this link differed between lowlands and highlands and depending on whether the system was at the gaining or retraction stage. This asymmetrical behaviour was likely caused by shifts in regional connectivity. Regional surface + groundwater storage compared well with water storage anomalies obtained from GRACE, suggesting that this tool may represent a methodological shortcut to estimate water storage changes. The tight connection between ground and surface water, and the relatively slow process of cumulative water accretion and coalescence of water bodies that precedes flood events offer the opportunity of developing warning systems that could help land managers to adapt to climate changes. Copyright © 2010 John Wiley & Sons, Ltd.

KEY WORDS water storage; groundwater dynamics; GRACE; surface water connectivity; flooding; water-table depth; plains

Received 3 December 2009; Accepted 6 June 2010

INTRODUCTION

Floods affect key ecological processes such as energy flow, nutrient cycling, and population dynamics, and are essential to maintain wetland and shoreline ecosystems (Galat *et al*., 1998; Caziani *et al*., 2001; Pringle, 2001; Johnson *et al*., 2005; Chaneton, 2006; De Loe, 2008). However, flood episodes not only affect natural ecosystems but also cultivated ones, threatening agricultural economy, transportation, infrastructure, and people's general well being (Viglizzo and Frank, 2006; De Loe, 2008). In flat, sedimentary landscapes with poorly developed regional drainage networks and groundwater close to the surface, flooding, and drought cycles involve changes in water-table depth that exert a significant influence on natural and managed ecosystems (Pringle, 2001; Schilling *et al*., 2004; Nosetto *et al*., 2009). On one hand, when the water table is shallow enough to supply moisture to plants, groundwater can become an important water source (Pratharpar and Qurseshi, 1998; Jobbágy and Jackson, 2004; Nosetto *et al*., 2009) that offers plants a second chance to use excess water stored during the rainy periods. On the other hand, when the water table is too close to the surface, vegetation growth can be negatively affected by waterlogging (Reicosky *et al*., 1985; Nosetto *et al*., 2009), which is particularly relevant in cultivated ecosystems. In addition, groundwater is tightly linked with surface water, and water table dynamics controls the formation and expansion of water bodies, determining the magnitude of flooding events (Winter, 1999; Brunke and Gonser, 1997; Toth, 1999; Ferone and Devito, 2004). In spite of this connection, the role of groundwater has been traditionally underemphasized (Pringle, 2001). Therefore, disentangling the groundwater–surface water interaction can help to understand the expansion–retraction dynamics of floods, anticipating their negative effects and taking advantage of the positive ones on both ecosystems and people (Pringle, 2001; Ferone and Devito, 2004).

Sub-humid alluvial and eolian plains, with a very extended and flat topography (regional slope <0·1%) such as that of Western Siberia, Hungary, Central Canada, and Southern South America (Jobbágy *et al*., 2008), display flooding cycles like the ones described above. The Western Argentinean Pampas is an example of such landscapes. The Pampas is a wide, sedimentary plain that encompasses more than 600 000 km^2 and corresponds,

* Correspondence to: E. G. Jobbágy, Grupo de Estudios Ambientales, IMASL, Universidad Nacional de San Luis/CONICET.
E-mail: jobbagy@unsl.edu.ar

for the most part, to cultivated land and pastured grasslands. Over the last 50 years, flood and drought episodes undermined the agricultural economy and human well being across this region (Fuschini Mejía, 1994; Viglizzo and Frank, 2006; Viglizzo *et al*., 2009). Because the succession of extreme events may become more frequent (Barros *et al*., 2006), quick adaptation measures will be increasingly demanded by the society. However, at the same time, contrary to the adverse effect expected on crop yields, floods are vital to maintain wetland ecosystems (Galat *et al*., 1998; Caziani *et al*., 2001; Pringle, 2001). Hence, extreme events (i.e. drought and floods) may have different consequences for managed and natural ecosystems. On one side, drought years are expected to have negative impacts on both cultivated vegetation and wetlands, but on the other side, floods may cause crop damage for waterlogging but are expected to have positive effects on wetland wildlife. This situation may pose a problem as different management objectives can lead to distinct strategies and at landscape scale, intermediate situations may represent a reconciling solution. Given that our interpretative picture is still incomplete both in agricultural and ecological terms, more research is needed to understand the expansion/retraction dynamics of floods to detect early warning signals and develop adaptation strategies.

The main goal of this study is to understand the dynamics of groundwater and its interaction with surface water bodies in the flooding Western Pampas of Argentina. Specifically in this paper, we (1) describe the dynamic of flooded area, groundwater (GW) depth, regional water storage, and precipitation throughout a regional flooding cycle, (2) explore the regional synchrony of these variables through time, and (3) study their reciprocal links at different spatial scales (i.e. site and region) by combining the analysis of GW depth and rainfall databases of more than 20 sites spread around a 28 000 km^2 region with radiometric (LANDSAT), interferometric (ENVISAT), and gravimetric (GRACE) remote sensing techniques.

METHODS

The study region

The study area corresponds to the western portion of the Argentinean Pampas and is known as Western or Inland Pampa (Soriano *et al*., 1991) (Figure 1). The area is a wide, aeolian, sedimentary plain that was shaped during the last Pleistocene glaciation (Aradas, 2002; Iriondo, 1999). It was originally occupied by native grasslands (Soriano *et al*., 1991), but currently it is dominated by annual crops and pastures, and represents one of the most productive areas of Argentina (Viglizzo and Frank, 2006; Baldi and Paruelo, 2008). The climate is temperate with annual temperature averaging 16·2 °C and mean annual rainfall of 980 mm (Diaz Zorita *et al*.,

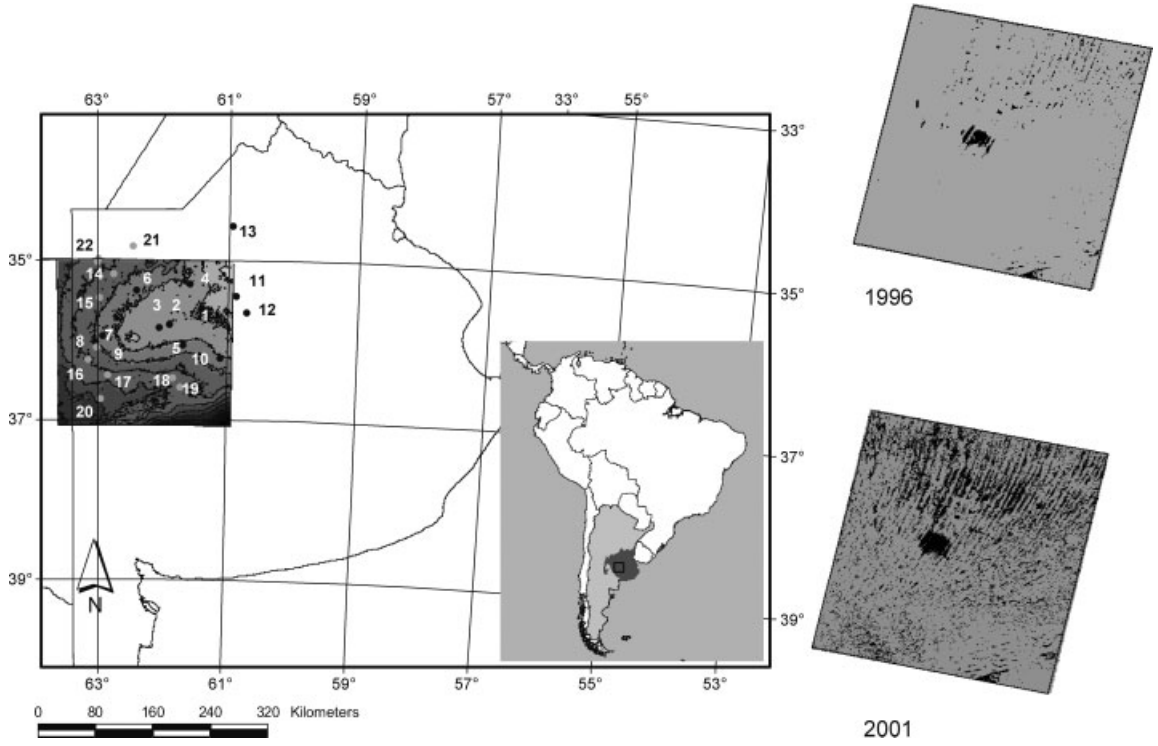

Figure 1. Study region. Left panel: Study area situated in the NW of Buenos Aires Province, Argentina. Square corresponds to LANDSAT scene 227–85, lines are level curves (10 m interval, beginning 80 masl, darker areas correspond to increasing elevation). Points corresponded to the 22 locations with phreatic data (black dots = lowlands sites, grey dots = upland sites): 1—Casares, 2—Pehuajó, 3—Paso, 4—M. de Hoz, 5—Biznaga, 6—Tejedor, 7—T. Lauquen, 8—Castilla Quince, 9—Castilla Casco, 10—Bolivar, 11–9 de Julio, 12—Dudignac, 13—Junín, 14—Tres Algarrobos, 15—América, 16—Pellegrini, 17—Tres Lomas, 18—La Paz, 19—Daireaux, 20—Salliqueló, 21—Ameghino, and 22—Villegas. Inset: Rio de la Plata grasslands in grey (Soriano *et al*., 1991). Right panels: Maps indicating the distribution of surface water (generated by the decision tree algorithm) in 1996 (2·7% of the area occupied with water), and 2001 (28%). The percentages were computed over the total area of the LANDSAT scene (28 000 km^2). Water bodies in black.

1998; Viglizzo *et al*., 2009). The humid to sub-humid climate and the extremely flat topography with a poorly developed regional run off system, make this region flood prone (Viglizzo *et al*., 1997; Chaneton, 2006; Viglizzo and Frank, 2006; Viglizzo *et al*., 2009). Rainfall is concentrated during the summer and the beginning of autumn with a pronounced decay during winter. In addition to intra-annual variability, drought and flooding episodes that severely affected crop production occurred during the last 50 years (Viglizzo and Frank, 2006). The soils are mostly Mollisols, deep and sandy, and the water table is close to the surface in all the territory (less than 5 m of depth) (Aradas *et al*., 2002). The region encompasses a very slight NW–SE topographic gradient of 0·05% (approximately 80 m in 300 km) and is characterized by the presence of shallow lagoons and ponds, and the lack of a river/stream network.

Data sources and analysis

We constructed a database with GW depth, area covered by water bodies (WB), and precipitation records (PPT). For groundwater and precipitation, we compiled existing data for 22 sites encompassing approximately 40 000 km^2 (Figure 1, Table I) with a temporal resolution that varied from weekly to monthly data. We summarized the data annually by averaging GW, or adding PPT from November of one year to October of the next from 1996 to 2005. In our analyses, each annual cycle was initiated in November at the start of the summer crop cycle, the most important of the region. The area and distribution of water bodies was characterized within the October–November period of each year using a LANDSAT scene (*see below*) that covers 28 000 km^2. Water table level data involved records from 22 shallow monitoring wells that reached phreatic groundwater. These observations were performed by the National Weather Service of Argentina (SMN), Cámara de Cereales, Instituto Nacional de Tecnología Agropecuaria (INTA), and private land owners. Not all the series were complete and the number of wells varied within the study period. Precipitation data were provided by Secretaria de Agricultura, Ganaderia, Pesca y Alimentos (SAGPYA). For the analysis at regional scale, in addition to the SAGPYA dataset, we also considered rainfall estimates from the TRMM online visualization and analysis systems (TOVAS) provided by NASA's Goddard Earth sciences (GES) data and information services center (DISC) (Kummerow *et al*., 1998; Su *et al*., 2008). Reference evapotranspiration (ETo) was calculated using Penman–Monteith method (Allen *et al*., 1998) with climatic variables available through SMN from five sites dispersed across the study area (Bolivar, Junín, Pehuajo, Villegas and 9 de Julio) (Table I). We later computed a climatic water balance as PPT-Eto.

To estimate water storage shifts, we considered surface and phreatic groundwater storage separately. To compute surface storage, we transformed our surface water coverage estimates (WB) to volume figures using an empirical relationship based on a high-resolution digital elevation model (vertical resolution = 0·1 m) covering 53 km^2 (59 214 data points) within an area that represents the typical aeolian landscapes of the region (Vedia: 34°21′LS; 61°36′LW). The point vector data were rasterized and

Table I. Study sites.

Site	Longitude	Latitude	Elevation	GW depth	Minimum	Maximum	Range	PPT	PCA WB	PCA GW	PCA PPT
Junin	−60·96	−34·59	75	−1·91	−1·10	−2·68	1·58	1056	0	0	1
Dudignac	−60·72	−35·66	76	−0·99	−0·44	−1·53	1·09	1070	0	1	0
9 de julio	−60·89	−35·46	77	−1·72	−1·07	−2·18	1·11	1038	0	1	1
Carlos Casares	−61·36	−35·63	81	−2·13	−1·46	−2·74	1·28	972	1	1	1
Pehuajo	−61·91	−35·82	84	−1·54	−1·35	−1·72	0·37	890	1	1	1
J. J. Paso	−62·07	−35·86	86	−1·39	−1·24	−2·05	0·81	890	1	1	1
Martinez de Hoz	−61·60	−35·32	87	−0·89	−0·18	−1·67	1·49	1099	1	1	0
Trenque Lauquen[a]	−62·73	−35·97	89	−2·07				1058	0	0	1
Bolivar	−61·12	−36·23	92	−2·21	−1·13	−3·83	2·7	942	0	1	1
La Biznaga	−61·70	−36·08	95	−1·58	−1·05	−2·18	1·13	1082	1	1	0
Carlos Tejedor	−62·42	−35·40	96	−1·75	−1·17	−2·35	1·18	1022	1	1	1
Castilla quince	−63·03	−36·11	100	−2·81	−1·62	−3·57	1·95	1058	1	0	1
Castilla casco	−63·04	−36·04	102	−0·97	−0·18	−1·72	1·54	1058	1	0	1
Tres Algarrobos	−62·77	−35·20	106	−2·16	−1·59	−2·54	0·95	917	1	1	0
America	−62·98	−35·49	108	−2·34	−1·71	−2·98	1·27	1045	1	1	1
Ameghino	−62·47	−34·85	111	−2·03	−1·87	−2·20	0·33	1100	0	0	1
Pellegrini	−63·15	−36·27	112	−3·47	−2·95	−4·17	1·22	848	1	1	1
Villegas	−63·02	−35·04	114	−2·33	−1·70	−2·49	0·79	1078	0	1	1
Tres Lomas	−62·86	−36·46	116	−2·68	−2·01	−3·18	1·17	828	1	1	1
Daireaux	−61·73	−36·60	117	−2·10	−1·64	−2·43	0·79	880	1	1	1
La Paz	−61·85	−36·49	117	−1·90	−1·01	−2·85	1·84	1043	1	1	0
Salliquelo	−62·96	−36·76	128	−1·86	−1·26	−2·57	1·31	846	1	1	1

Name, geographic coordinates (decimal degrees), elevation (masl), average, minimum, maximum, and range of GW depth (meters from the surface), and average precipitation (mm/year) are indicated for each site. PPT and GW corresponds to the overall annual average considering November–October period. The sites that were included (1) or not (0) in PCA for coverage of WB, GW depth, and PPT.
[a] GW depth is available only for 1995–1996 and 1996–1997.

interpolated at 30 m of pixel size. From this digital elevation model, we removed the regional slope by using the altitudinal residuals from a regression of elevation versus longitude and latitude ($r^2 = 0{\cdot}14$, $p < 0{\cdot}01$) using a procedure similar to Nosetto *et al*. (2009). Even under the slight regional topographic gradients of the Western Pampas, absolute elevation is not sufficient to capture the relative position (upland–lowland) of a particular point in the landscape. Given that the same absolute elevation could correspond to a lowland or an upland as we displace across the regional gradient, we used the elevation residuals from this gradient as a better way to describe the relative position of points across the local topographic gradient between the bottom of lowlands to the top of uplands. Using these residuals, we calculated surface water volume increase with raising water levels that ranged from the lowest altitudinal residual to the highest altitudinal residual found in the scene. By doing this, we assumed a progressive increase of the flooded area obtaining its associated shift in the water column height above the surface of each pixel (i.e. water thickness) and integrated their volumes for the whole scene. Absolute flooded area was converted to percentage of flooded area and surface water volume to mean water thickness for the whole area. We obtained an empirical 'surface-volume' function linking these two variables (Figure 2) that was then applied to the whole region.

In addition to the previous approach, we established an independent 'surface-volume' function based on local satellite observations at a single large depression and its associated water body (Las Tunas-Hinojo: 35°58′LS; 62°26′LW) in which surface water height measurements were obtained based on ENVISAT radar data. ENVISAT

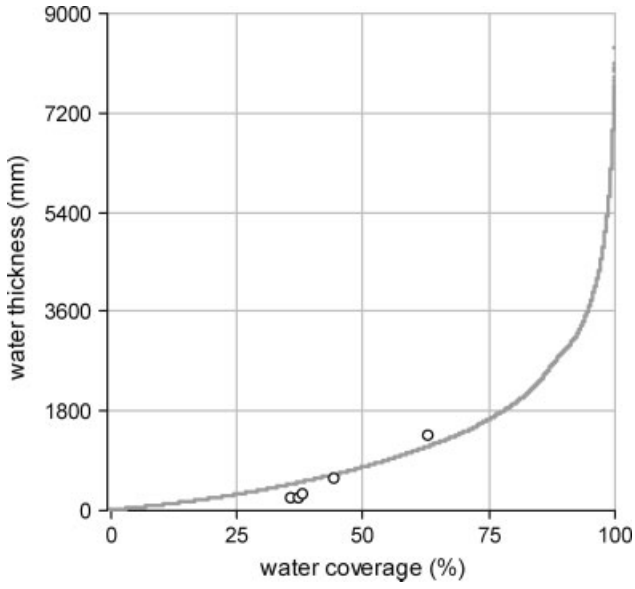

Figure 2. Relationship between the proportion of the land covered by surface water bodies and their water storage, characterized as the mean water thickness that they represent for the whole area. The line represents a function obtained using a detailed digital elevation model for a representative section of the study region, whereas the dots correspond to remote sensing estimates (LANDSAT for surface water coverage and ENVISAT for water level) at the Las Tunas-Hinojo lake and surrounding areas.

is a radar-altimetric mission operated by European Space Agency (ESA) since 2002, and as other radar satellites, uses the two-way time delay between the microwave pulse emission and the ecoreception to deduce the height of the surface topography (Birkett *et al*., 2002; Frappart *et al*., 2006). As it is a nadir instrument, a time series of water height variation can be constructed only if the orbit of the satellite passed over the target water body or landscape feature. The 'surface-volume' functions obtained by both methods were highly convergent (Figure 2). Phreatic groundwater storage was defined as the amount of water stored in the saturated zone above an arbitrary reference level. Groundwater storage shifts were calculated as the product of level differences (GW depth date$_i$—GW depth 1996) and a typical specific yield figure for unconfined aquifers on sandy aeolian sediments. Specific yield in this case corresponds to the proportional volume of the sedimentary matrix that is occupied by water between field capacity to saturation potentials. In our case, it was assumed to be 20% based on global values for aeolian sediments (Dingman, 1993) and local values for other locations within the same sedimentary material in the Pampas (Aradas *et al*., 2002). To evaluate the sensitivity of our surface water storage estimates to the 'surface-volume' function parameters, we computed storage differences after shifting terrain slopes in the digital elevation model by ±25% and adjusting 'surface-volume' functions accordingly. This range encompasses the variability of slopes along this region. Similarly, we explored groundwater storage shifts after changing specific yield values by ±25% that includes the ranges described for aeolian sediments (Dingman, 1993). Finally, we computed total regional water storage as the sum of surface water and groundwater storage per year.

We took advantage of our water storage estimates to evaluate the potential use of the gravity recovery and climate experiment (GRACE) (Rodell and Famiglietti, 2002; Tapley *et al*., 2003) in our study system. GRACE twin satellites measure changes in the distribution of mass over the Earth that in turn causes changes in the Earth gravity field. Terrestrial water storage variations are the main cause of month to month fluctuations in gravity field, and therefore GRACE records can be used to track changes in surface and groundwater storage in hydrologic reservoirs (Tapley *et al*., 2003; Swenson *et al*., 2003). GRACE data were expressed as 'equivalent of water thickness' (originally in centimetre) with respect to an historical mean (i.e. negative values indicate drying conditions). GRACE measurement accuracy varies depending on spatial scale, degree of smoothing and latitude, and ranges from 3 to 10 mm (Swenson *et al*., 2003). Our analysis compared GRACE estimates of water storage shifts versus our own estimates of surface water and groundwater storage shifts, ignoring any contribution from unsaturated water storage. In the Pampas, where hydrological monitoring networks are virtually nonexisting, GRACE data could greatly improve flood observation and warning strategies thereby reducing the need of other remotely

sensed or phreatimetric data and simplifying the computation of water storage shifts.

We performed our analyses at two spatial scales: regional and site scale. We used simple linear regression after checking for normality of residuals and nonparametric Spearman correlation to describe the relationship among precipitation, surface water coverage, and GW depth. To assess the synchronicity of each one of these variables across sites, we performed a principal component analysis (PCA) using site to site correlation matrix. Higher synchronicity would result in a clear separation of years, and hence higher eigenvalues associated to the first and second axes. By looking at the eigenvectors, this analysis has also the ability to identify groups of sites with similar temporal behaviour.

Surface water detection

Surface water bodies were differentiated from surrounding vegetation (both natural and cultivated) and bare soil, and mapped through image classification procedures based on a decision tree (Friedl and Brodley, 1997). We first performed an unsupervized classification through the *k*-means algorithm available in ENVI 4·2 using 20 classes that we later clustered into four: clear water, turbid water, vegetation, and areas with bare or salty soils. To build the water body spectral signature, we used the map generated by this classification and chose ten polygons that met two conditions: first, they were easily identified into the LANDSAT scene, and second, each polygon was at least of 5×5 LANDSAT pixels (150×150 m). In addition, we chose five polygons of each of the rest of the classes. Based on this information, we obtained the spectral signatures of these four classes that we later clumped in water versus no-water classes. We used a principal component analysis to identify the bands that were more useful in separating these classes. Based on this analysis and on a graphical representation of the spectral characteristics of each class, we built the decision tree algorithm that considered Normalized Difference Vegetation Index (NDVI, infrared − red/infrared + red) (i.e. LANDSAT bands 4 and 3, respectively), and LANDSAT bands 5 and 7 (median infrared and long infrared).

We worked with 10 LANDSAT scenes (path 227, row 85) corresponding to October or November of each year from 1996 to 2005. We explored the success in the detection of water bodies using QuickBird scenes from 2003 available on Google Earth, finding a strong agreement (i.e. more than 90% of the water bodies were successfully detected by our 2003 map).

RESULTS

Regional flooding cycle

Throughout the 10-year period of our study, a full-flooding cycle was captured. Regional flooded area expanded and mean water-table levels raised, peaking in 2001 and retracting rapidly in the next 2 years (Figure 3a). The proportion of the region that was flooded expanded from 2·7% (700 km^2) at the beginning of the study period to 28% (7157 km^2) in 2001, encompassing ∼21 000 and ∼162 000 individual water bodies, respectively (Figure1). Regionally, averaged GW depths displayed ∼2·5 m level raise during this flooding cycle with depth from the surface ranging from 3·7 m at the beginning of the study period to 1·2 m in 2001. Water-table levels declined ∼0·9 m in the next 3 years but remained more than 1·5 m above the initial levels for the rest of the observation period. At the regional scale, groundwater levels paralleled flooded area dynamics (Spearman $r = 0{\cdot}89$, $p < 0{\cdot}01$) (Figure 3a). Whereas, water-table level shifts are likely to be well represented by our network of sites, mean absolute groundwater levels throughout the region are probably closer to the surface given that the location of most monitoring wells is usually biased towards higher landscape positions.

Regional water storage raised by ∼800 mm between 1996 and 2001. Sixty-three percent of this water accretion (∼500 mm) was stored as groundwater and the rest (∼300 mm) as surface water bodies (Figure 3b). At the end of the study period, the region had a net gain of ∼490 mm mostly explained by groundwater storage. The fastest net water accretion and loss rates took place during 1999–2000 (277 mm/year) and 2002–2003 (−219 mm/year). The sensitivity of these figures to changes in our assumptions on sediment-specific yield and topographic configuration indicates that at the peak of the flooding cycle, a 25% increase/decrease of specific yield values (i.e. from 15% to 25%) would result on water storage shifts of ±128 mm; whereas, a shift in the flooded area versus surface water storage function based on a 25% increase/decrease on average slopes would imply water storage shifts of ±75 mm, respectively.

Precipitation and climatic water balance (precipitation—reference evapotranspiration) temporal variation explained in part the onset and retraction of the flooding cycle. Annual precipitation (November–October) averaged 995 mm, ranging between 790 (2002–2003) and 1210 mm (2000–2001) with a temporal coefficient of variation of ∼20% throughout the study period (Figure 3c) Annual ETo averaged 1120 mm and was highly stable, displaying a coefficient of variation of 5%. Regionally, we found a strong association between annual shifts in water storage and climatic water balance (Table II). In addition, annual precipitation and ETo were significantly related to flooded area, but they did not account for the variability in GW depth (Table II). Precipitation and ETo were also associated to total water storage (Table II).

Spatial variability

Although the study region displayed a clear wave of water-table raise and flooding as a whole, differences in the magnitude and timing of this wave emerged when sites were analysed individually. Consistent contrasts between highland and lowland sites became evident

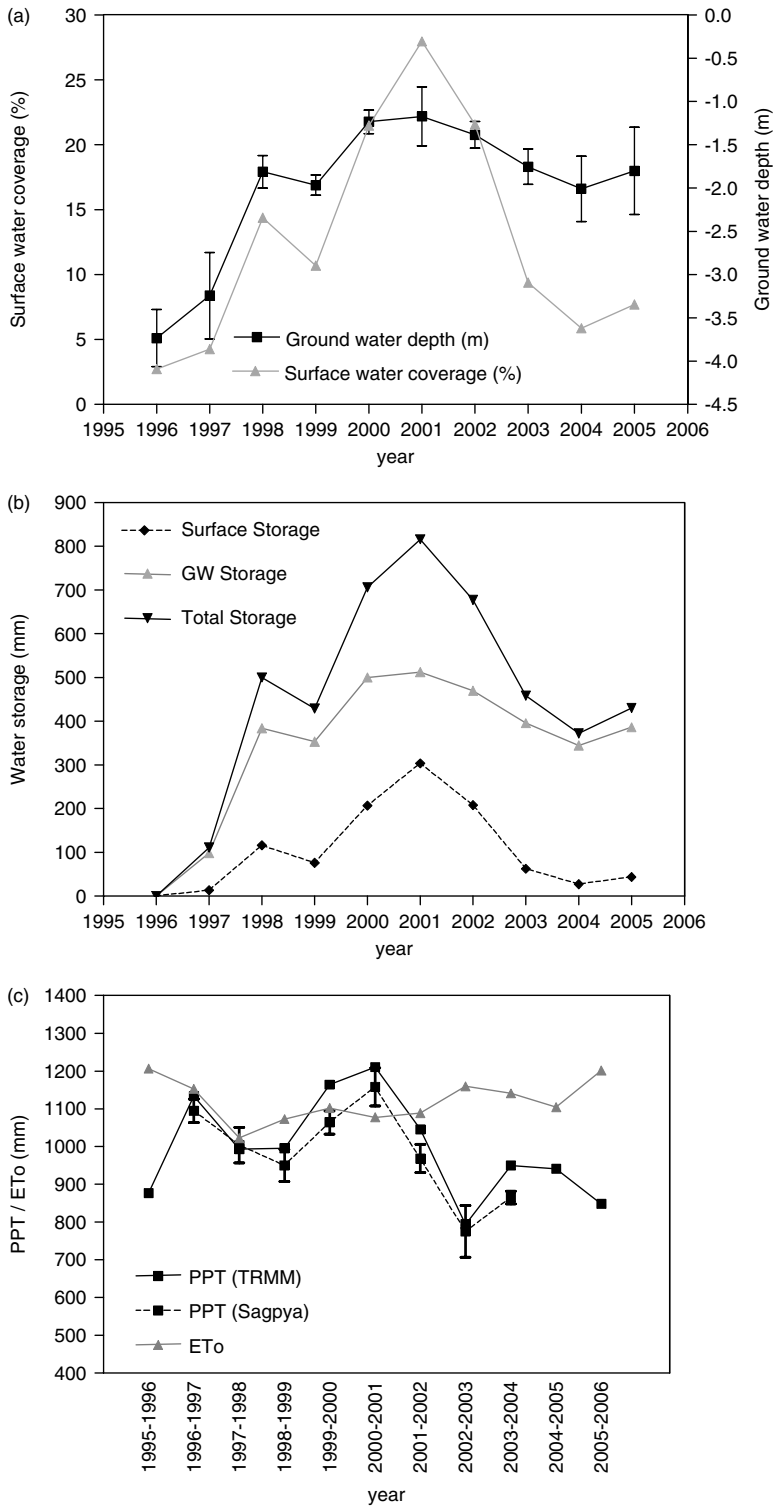

Figure 3. Hydrological shifts throughout the flooding cycle. (a) Fluctuation of regional surface water coverage and groundwater depth from the surface. Bars represent standard errors. (b) Surface, groundwater, and total regional change in storage. (c) Precipitation and reference evapotranspiration. Annual values correspond to November–October periods.

in this analysis. Average and maximum flooded area increased towards low-elevation sites ($R^2 = 0{\cdot}67$ and $0{\cdot}62$, $p < 0{\cdot}01$) and, paralleling this trend, groundwater levels were closer to the surface ($R^2 = 0{\cdot}26$, $p < 0{\cdot}05$). Sixty percent of the sites experienced peak flooding in 2001, whereas, the remaining 40% peaked in the previous or following year. Water tables were closer to the surface in 2001–2002 for 64% of the sites, and in either 2000–2001 or 1997–1998 for the rest of them.

Throughout the study period, sites showed decreasing levels of synchronicity for their flooded area, GW depth, and rainfall, respectively, as indicated by site to site correlations and ordination analyses. Correlations in the temporal series of these three variables across all

Table II. Spearman r correlation coefficients.

	PPT	ETo	PPT-ETo
Flooded area	**0·612**	**−0·745**	**0·612**
GW	0·466	−0·442	0·479
WS total	0·540	−0·600	0·588
Delta WS	0·452	−0·619	**0·738**

Underlined: 1 significant values at p<0.1; in bold: significant values at p<0.05. Flooded area from 1996 to 2005, GW depth corresponds to the month closer to the date of each Landsat scene, Delta WS: delta water storage computed as the WS yearx- WS yearx-1; PPT and ETo correspond to annuals values from November to October of each year

individual pairs of sites were significant ($p < 0{\cdot}05$) in 75, 28, and 21% of the cases for flooded area, GW depth and rainfall, respectively (Tables III–V). Correlations for flooded area were higher among lowland sites with 90% of the comparisons being significant.

Ordination of years based on flooded area at different sites showed a clear separation of 2001, representing the peak of flooding in most sites (Figure 4a). The first axis of the PCA ordered the years based on their average value across sites (i.e. flooded area in 2001, 2000, 2002, and 1998 with negative scores, were above the overall mean, whereas, the opposite was true for 1999, 2003, 2005, 2004, 1997, and 1996) and accounted for 74% of the variability. The site eigenvectors for this axis, which can be taken as the correlation coefficients between scores for years and site values (i.e. flooded area) were all negative and similar in magnitude. This and the fact that the first axis explains such a high proportion of the variability, highlights the synchronous surface water dynamics among sites. The separation of the years in the second axis (12% of the variability) was mainly accounted by the surface water dynamics of two groups of sites: Salliquelo, América, Tres Lomas, and Castilla had a pronounce peak in 2001, whereas, in Daireaux, La Paz, Paso, and La Biznaga, the period of maximum flooding was more distributed throughout 2000, 2001, and 2002 (Figure 4a inset). These two groups were associated broadly with West–East coordinates (Figure 1) ($r = -0{\cdot}72$, $p < 0{\cdot}01$ for the correlation of geographic longitude versus eigenvectors axis II). With the exception of La Paz and Daireaux, the distinction between negative and positive eigenvectors for axis II was associated with highland (positive) and lowland (negative) positions. Overall, this distinction across sites indicates a well-defined flooding peak towards the highest sites of the West (six of the eight highland sites had their maximum flooded area in 2001), and a more distributed and persistent flooding towards the lower sites of the East (with peaks in 2000, 2001, and 2002).

Ordination of years based on depth to groundwater also indicated synchronicity among sites but to a lower extent than that observed for flooded areas (Figure 4b). The first axis of the ordination accounted for 55% of variability and it was related with the mean values across sites (i.e. 2001–2002, 2000–2001 and 1997–1998 had GW depth below the mean). Although the peak years were partly coincident among sites, there were many differences in their dynamics with Pehuajó as the most distinct site (Figure 4b inset). Pehuajó showed a more stable dynamics with no clear distinction of minima and maxima, whereas, Daireaux, Tejedor, and 9 de Julio showed bimodal curves with peaks in 1997–1998 and 2001–2002. As occurred with ordination of flooding data, eigenvectors for the first axis were all negative but had a higher range of values. This also is an indication of the similarity in groundwater dynamics among sites. Sites with positive eigenvectors for axis II corresponded to minimum depths occurring in 2001–2002, whereas, sites with negative eigenvectors recorded their minimum in 1997–1998, yet there was no clear distinction between lowland and highland sites for this variable (Figure 4b inset). Overall, groundwater dynamics showed some similarities between sites (i.e. 2001–2002 was the peak year for 60% of the sites), but there were some distinct patterns that were not clearly associated with site elevation or coordinates.

The first axis of the ordination based on rainfall values (from November to October) accounted for 56% of variability, and it was related to average values across sites (i.e. in 2000–2001, 1996–1997, 1999–2000, 1997–1998, and 2001–2002 rainfall was above the overall mean) (Figure 4c). As occurred with the ordination of flooding and groundwater data, the first axis eigenvectors were all negative and of a similar magnitude. This is also an indication of the relatively coincident rainfall dynamics. The second axis was associated with the year of the minimum (1998–1999 represented the year of the minimum in Casares, Ameghino, and M. de Hoz, whereas, Pellegrini, Tres Lomas, Villegas, and Daireaux represented their minimum values in 2002–2003 or 1995–1996) and accounted for 17% of the variability (Figure 4c inset). The site eigenvectors for this axis were negatively correlated with elevation and positively correlated with longitude ($r = -0{\cdot}71$ and $0{\cdot}74$, $p < 0{\cdot}01$). The peak of precipitation occurred in 2000–2001 for 40% of the sites but 20% had their peak in 1996–1997. Overall, compared to flooded area dynamics, rainfall showed a lower degree of synchrony among sites.

Cross correlations

Regionally, water table paralleled flooded area dynamics, but the correlation between these variables differed across sites, with highlands showing a more simultaneous variation and lowlands showing a lagged dynamics of GW depth with respect to flooded area. When current flooded area and GW depth were considered, significantly positive correlation were observed at most highland sites and at the lowland site of Pehuajó (Table VI). When lags were explored, a significant ($p < 0{\cdot}10$) association of GW depth in the current year to flooded area on the previous emerged in five lowland sites and three highland sites (Table VI). The relationship between these two variables with rainfall also differed across sites with a positive correlation between flooded area and

Table III. Site to site Spearman r correlation coefficients for the area occupied by water bodies.

	Casares	Pehuajó	Paso	Hoz	Biznaga	Tejedor	Castilla Q	Castilla C	Tres Algarrobos	América	Pellegrini	Tres Lomas	Daireaux	La Paz	Salliquelo
Casares	1·00														
Pehuajó	**0·87**	1·00													
J. J. Paso	**0·72**	0·58	1·00												
M. de Hoz	**0·85**	**0·75**	0·60	1·00											
Biznaga	**0·92**	**0·80**	**0·85**	**0·70**	1·00										
C. Tejedor	**0·87**	**0·70**	**0·90**	**0·77**	**0·92**	1·00									
Castilla Q	**0·78**	**0·73**	**0·88**	**0·70**	**0·88**	**0·90**	1·00								
Castilla C	0·63	**0·77**	**0·72**	0·63	**0·73**	**0·72**	**0·92**	1·00							
Tres Algarrobos	**0·75**	**0·83**	0·48	0·52	**0·73**	**0·70**	**0·72**	**0·70**	1·00						
America	**0·75**	**0·90**	0·55	0·53	**0·73**	**0·68**	**0·75**	**0·77**	**0·97**	1·00					
Pellegrini	**0·75**	**0·68**	**0·83**	0·62	**0·87**	**0·88**	**0·98**	**0·88**	**0·77**	**0·77**	1·00				
Tres Lomas	**0·77**	0·55	**0·83**	**0·68**	**0·80**	**0·83**	**0·88**	**0·73**	0·53	0·53	**0·87**	1·00			
Daireaux	0·62	0·32	**0·70**	0·60	**0·68**	**0·70**	0·65	0·50	0·23	0·18	0·62	**0·87**	1·00		
La Paz	**0·78**	0·53	**0·77**	**0·78**	**0·83**	**0·82**	**0·70**	0·52	0·32	0·30	0·63	**0·73**	**0·83**	1·00	
Salliquelo	**0·82**	**0·82**	0·60	**0·70**	**0·76**	**0·73**	**0·82**	**0·82**	**0·84**	**0·84**	**0·82**	**0·82**	0·58	0·50	1·00

Sites are ordered from low to high altitude. Underlined: significant values at $p < 0{\cdot}1$; in bold: significant values at $p < 0{\cdot}05$, underlined and in bold: significant values at $p < 0{\cdot}01$. Sites 1–7 correspond to lowlands.

Table IV. Site to site Spearman r correlation coefficients for GW depth.

	Dugignac	9 de Julio	Casares	Pehuajó	J. J Paso	M. de Hoz	Bolivar	Biznaga	Tejedor	Tres Algarrobos	América	Pellegrini	Villegas	Tres Lomas	Daireaux	La Paz	Salliquelo
Dugignac	1·00																
9 de Julio	**0·96**	1·00															
Casares	0·61	0·50	1·00														
Pehuajó	0·07	−0·14	0·18	1·00													
J. J. Paso	0·37	0·37	−0·03	**0·83**	1·00												
M. de Hoz	**0·93**	**0·89**	0·82	0·07	0·14	1·00											
Bolivar	**0·93**	**0·89**	0·57	0·25	0·49	**0·89**	1·00										
Biznaga	0·66	0·66	0·26	0·49	0·37	0·54	0·71	1·00									
Tejedor	**0·86**	**0·89**	0·32	0·11	0·71	0·79	**0·89**	**0·83**	1·00								
Tres Algarrobos	0·57	0·43	0·46	0·79	0·60	0·57	0·71	0·77	0·61	1·00							
América	0·66	0·66	0·26	**0·83**	**0·89**	0·49	0·71	0·71	**0·94**	**0·83**	1·00						
Pellegrini	0·00	−0·07	−0·54	0·57	**0·83**	−0·25	0·07	0·43	0·25	0·39	0·71	1·00					
Villegas	0·00	−0·04	−0·64	0·36	0·60	−0·32	0·00	0·49	0·18	0·25	0·54	**0·93**	1·00				
Tres Lomas	0·25	0·04	0·14	**0·89**	**0·89**	0·14	0·29	0·71	0·21	0·79	1·00	0·68	0·57	1·00			
Daireaux	**0·86**	**0·89**	0·32	0·11	0·71	0·79	**0·89**	**0·83**	**0·99**	0·61	**0·94**	0·25	0·18	0·21	1·00		
La Paz	0·61	0·46	0·36	0·75	0·71	0·54	0·68	**0·83**	0·64	**0·96**	**0·94**	0·54	0·43	**0·86**	0·64	1·00	
Salliquelo	0·50	0·36	0·18	0·79	**0·89**	0·39	0·57	0·71	0·61	**0·89**	1·00	0·71	0·57	**0·89**	0·61	**0·96**	1·00

Sites are ordered from low to high altitude. Underlined: significant values at $p < 0{\cdot}1$; in bold: significant values at $p < 0{\cdot}05$, underlined and in bold: significant values at $p < 0{\cdot}01$. Sites 1–9 correspond to lowlands.

Table V. Site to site Spearman r correlation coefficients for rainfall.

	Junin	9 de julio	C. Casares	Pehuajó	T. lauquen	M. de Hoz	Bolivar	Tejedor	América	Ameghino	Pellegrini	Villegas	Tres lomas	Daireaux	Salliquelo
Junin	1·00														
9 de julio	0·45	1·00													
C. Casares	**0·77**	**0·74**	1·00												
Pehuajó	0·63	**0·71**	**0·87**	1·00											
T. lauquen	0·58	**0·72**	**0·72**	0·67	1·00										
M. de Hoz	0·55	0·48	0·55	0·60	0·20	1·00									
Bolivar	**0·77**	0·69	**0·93**	**0·82**	0·57	0·42	1·00								
Tejedor	**0·83**	0·69	**0·92**	**0·75**	**0·83**	0·47	**0·80**	1·00							
América	0·25	0·19	0·38	0·68	0·45	**0·72**	0·22	0·33	1·00						
Ameghino	0·52	0·45	0·65	**0·78**	0·20	**0·80**	0·63	0·40	0·63	1·00					
Pellegrini	−0·02	−0·10	0·23	0·18	**0·73**	−0·02	−0·01	0·39	0·38	−0·23	1·00				
Villegas	0·23	0·00	0·20	0·53	0·47	0·57	0·02	0·27	**0·93**	0·43	0·41	1·00			
Tres lomas	0·28	−0·05	0·28	0·33	**0·85**	0·03	0·08	0·53	0·47	−0·15	**0·85**	0·62	1·00		
Daireaux	0·00	0·07	0·45	0·53	0·62	0·15	0·33	0·30	0·53	0·35	0·64	0·40	0·45	1·00	
Salliquelo	0·40	0·19	0·53	0·73	0·63	0·60	0·43	0·48	**0·90**	0·57	0·49	**0·80**	0·57	0·62	1·00

Sites are ordered from low to high altitude. Underlined: significant values at $p < 0{\cdot}1$; in bold: significant values at $p < 0{\cdot}05$, underlined and in bold: significant values at $p < 0{\cdot}01$. Sites 1–8 correspond to lowlands.

precipitation of the corresponding year in five out of seven lowland sites and in two out of nine highland sites (Table VI). As it occurred at the regional scale, the association between precipitation and GW depth was weaker than that with flooded area with only three sites with significantly positive correlations at $p < 0{\cdot}10$ (Paso, La Biznaga, and Ameghino). When lags were explored, a significant association of GW depth of the current year to precipitation of the previous year emerged in seven sites, most of them were lowlands. However, the relationship between flooded area and precipitation did not improve when a lag was considered (Table VI).

Evaluation of satellite gravity data

Regional water storage in the saturated zone and surface water bodies compared well with terrestrial water storage anomalies obtained from remotely sensed gravitational data (time series of average values obtained from GFZ data base, 400 km resolution for four pixels corresponding to the study area) (Figure 5). Although we only counted with few comparable dates, the two data series coincided in showing a decline during February 2004 and a recovery between March and August 2004. With the exception of November 2004, the estimation of regional storage based on these two independent sources was coincident ($R^2 = 0{\cdot}41,\ p < 0{\cdot}05$). However, the changes in storage estimated by GRACE were consistently higher than the ones estimated from surface water area and groundwater level variations (i.e. the slope of the regression line <1, Figure 5 inset).

DISCUSSION

GW depth and surface water coverage showed marked changes in sedimentary, very flat landscapes such as Western Pampas. During the 10-year period studied, surface water increased tenfold, covering more than one fourth of the analysed region, whereas, groundwater storage changed by approximately 400 mm, which represent between 30% and 50% of the water that enters the system as precipitation annually. Observed groundwater level shifts (2·5 m) matched well with those calculated for surface water bodies (2·7 m) based on our surface-volume analysis. Although groundwater is often perceived as a relatively static reservoir (Alley *et al.*, 2002; Sophocleous, 2002), its most superficial component represents not only a strong contribution to the interannual variation of total water storage in this type of landscapes, but also shows rapid storage shifts (146 mm between 1999 and 2000) that are tightly linked to surface water coverage.

Although ground and surface water are tightly linked, their timing of changes seems to differ depending on whether the system is at the water gaining or the water loss phase. When the region was gaining water, annual storage shifts were more pronounced for groundwater than for surface water (Figure 3b). The opposite was true in the water loss phase, when surface water displayed a more pronounced shift than groundwater. This

asymmetrical behaviour can be explained by a differential predominance of ground to surface water fluxes and also by changes in the hydrological connectivity throughout the landscape (Ward *et al*., 2002; Smerdon *et al*., 2005; Martin and Soranno, 2006, Jackson *et al*., 2009). In addition, evaporative water losses can achieve higher rates for surface water bodies than groundwater, given that year-round tank evaporation usually exceeds the potential evapotranspiration of the typical crop and pasture covers of the Pampas (Viglizzo *et al*., 2009).

Although complex and highly variable in time and space, the direction and importance of water transport between groundwater and surface reservoirs changed in a relatively consistent way during the flooding cycle that we studied (Figure 6). Results suggest that at the beginning of the flooding cycle there was a widespread groundwater elevation and consequently, rapid changes in groundwater storage. Surface water coverage increased through the expansion of water bodies that were already present, but primarily by the development of new ones. In this stage, groundwater to surface water movements were predominant and local transport prevailed. As excess water accumulated, water bodies became larger and eventually collapsed and merged (Aradas *et al*., 2002). A connection threshold was identified (in our study period achieved on year 2001) beyond which surface water

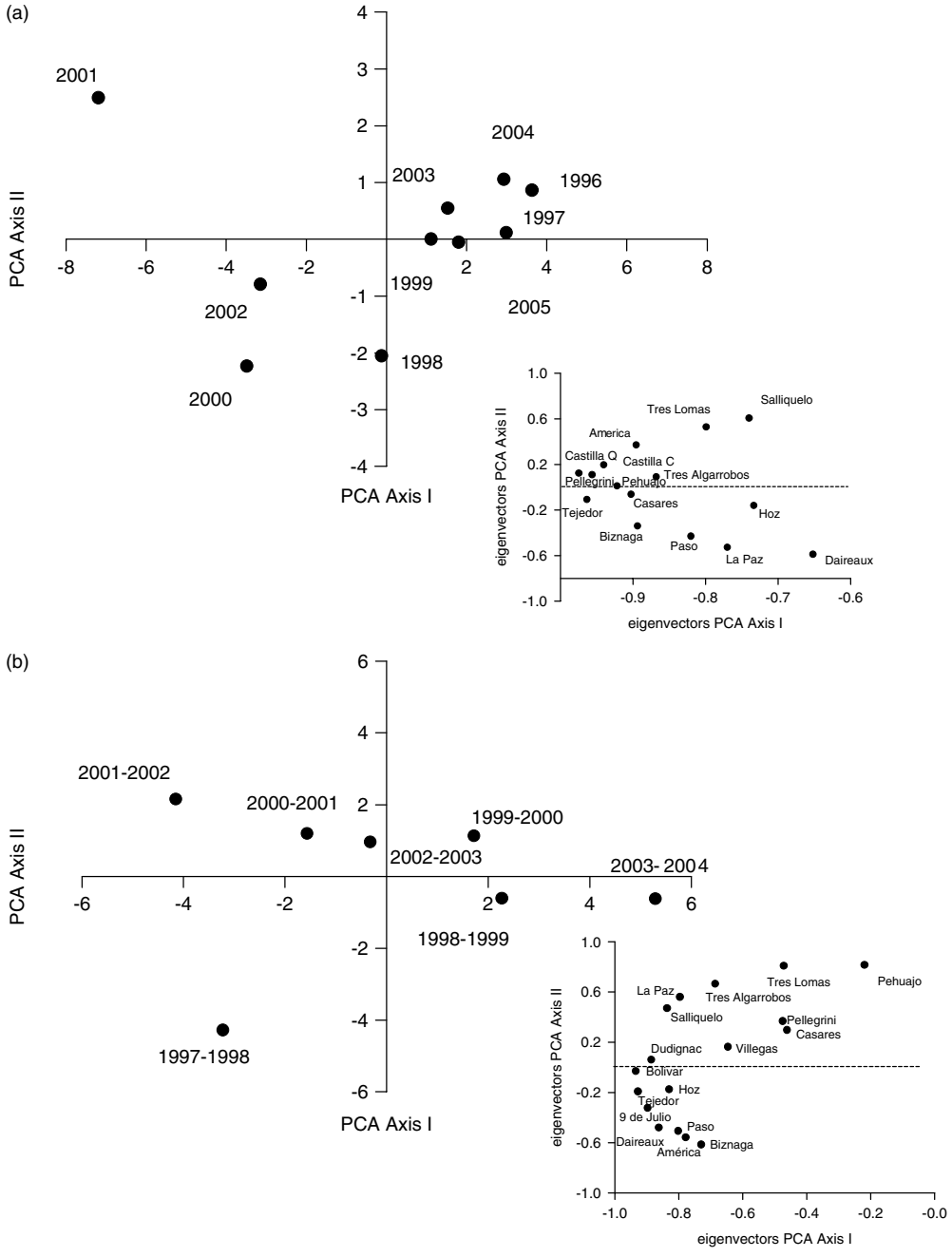

Figure 4. Ordination of years based on (a) water bodies, (b) groundwater depth, and (c) rainfall dynamics. Main Panels: Ordination of years in the PCA multivariate space. Inset: Axis I and II Eigenvectors scaled to standard deviation (they can be taken as the correlation coefficient between scores for years and sites).

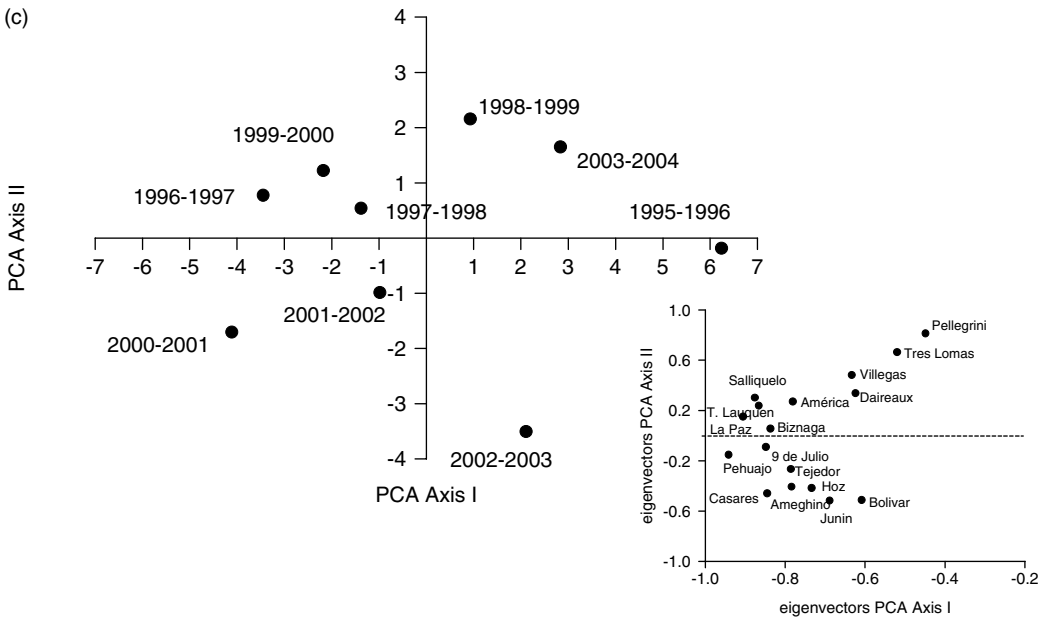

Figure 4. (*Continued*).

Table VI. Cross correlations within sites for each pair of variables.

Site	WB-GW	WB_{x-1}–GW	WB–PPT	WB–PPT_{x-1}	GW–PPT	GW–PPT_{x-1}	Delta GW–PPT
Junín					0·25	**0·78**	0·77
9 de julio					0·35	0·53	0·38
C. Casares	0·10	0·77	**0·66**	0·54	0·14	**0·82**	**0·83**
Pehuajó	**0·86**	0·43	0·62	0·62	0·28	0·35	0·43
J. J. Paso	0·65	0·70	0·62	0·14	0·77	0·48	0·70
M. de Hoz	0·50	**0·83**	0·62	0·12	0·18	0·14	0·31
Bolivar					0·26	**0·86**	**0·68**
La Biznaga	0·53	**0·99**	0·43	0·48	0·66	0·03	**0·78**
Tejedor	0·53	**0·83**	0·47	0·50	0·07	**0·85**	0·71
Castilla Quince	0·70	**0·99**	0·59	0·53	0·80	0·71	0·20
Castilla Casco	0·70	**0·99**	0·52	0·33	0·60	0·77	0·70
Tres algarrobos	0·68	**0·83**	0·06	0·52	−0·32	0·53	0·25
América	**0·94**	0·50	0·21	0·45	0·31	0·37	0·70
Ameghino					0·77	−0·08	0·30
Pellegrini	**0·93**	0·48	0·15	0·68	0·28	0·60	0·66
Villegas					0·57	**0·78**	0·66
Tres lomas	0·57	**0·83**	0·53	**0·83**	0·21	0·46	0·60
Daireaux	0·42	0·54	**0·70**	0·23	0·43	0·53	0·37
La Paz	**0·69**	0·63	**0**·63	0·60	0·31	**0**·63	**0·82**
Salliquelo	**0·87**	0·69	0·48	0·54	0·28	0·53	**0·94**

Values are Spearman r correlation coefficients. Underlined: significant at $p < 0{\cdot}1$, bold: $p < 0{\cdot}05$, bold and underlined: $p < 0{\cdot}01$. Sites are ordered from low to high elevation. N is variable across sites (between 6 and 11). Sites 1–10 correspond to lowlands. The suffix $x - 1$ refers to the value of each variable in the previous year (e.g. WB–PPT_{x-1} refers to the correlation between WB of the year x, and PPT of the year $x - 1$).
WB, coverage of water bodies; GW, groundwater depth; PPT, precipitation.

connectivity drastically changed and regional surface water transport from higher to lower areas occurred (Figure 6). This can explain the more extended peak (until 2002) in many of the lowland sites for both surface water area and groundwater level. Contrary to the earlier stage, regional transport gained importance at this time. It has been shown that the position of surface water bodies in the landscape (i.e. highland versus lowland) affects the velocity and dynamic of water fluxes as well as hydrological connectivity, that in turn can affect multiple attributes such as water chemistry and clarity (Poole *et al*., 2002; Ferone and Devito, 2004; Martin and Soranno, 2006). At the retraction period, groundwater declines lagged behind surface water cover changes. This was more marked in lowland sites, likely due to their higher accumulation of surface water (Figure 6). Faster surface water declines can also be attributable to more rapid evaporative water losses (Figure 6) (Winter, 1999). In this last stage, net water transport occurred from groundwater to surface water, and again it was restricted to local scale. The construction of channels during the years of maximum flooding, often following an anarchic

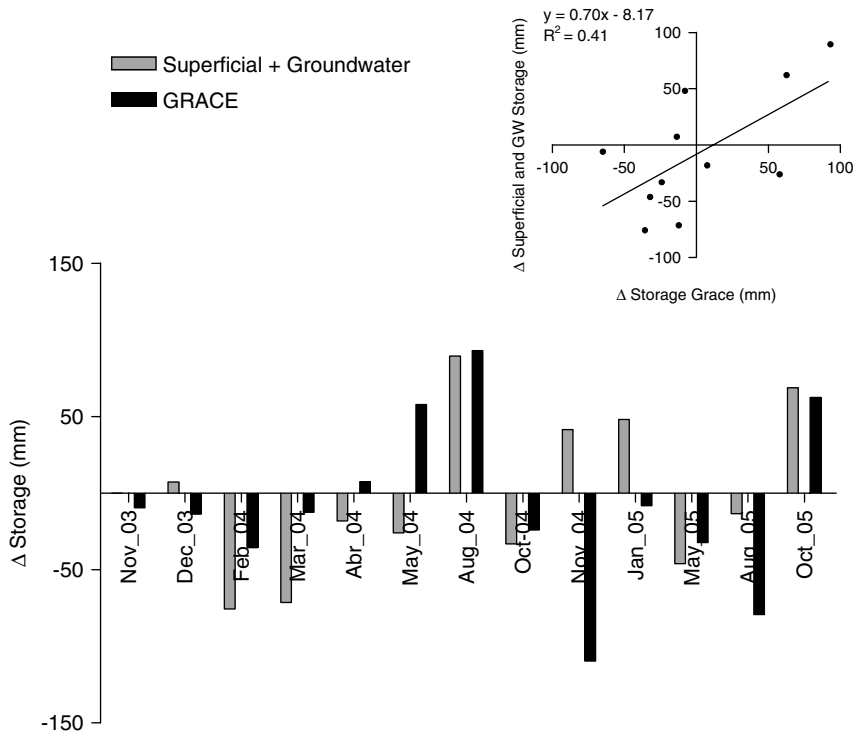

Figure 5. Differences in water storage between two consecutive dates from November 2003 to October 2005 estimated using surface water coverage shifts + variations in groundwater depth and GRACE time series. Negative values indicate decay in water storage (note that the time series for surface + groundwater was not complete and therefore the periods vary in length). Inset: relationship between △ Storage estimated with the different datasets.

response to the emergent threats to infrastructure, could have amplified surface water transport at peak flood, favouring the asymmetrical behaviour of raising and declining periods. Any hydrological management plan should specifically consider this dynamic behaviour to forecast floodings and minimize their potential negative effects (Pringle, 2001; Chaneton, 2006).

Although lateral movements of water are assumed to be negligible in areas with very low topographic gradient (<0·1%) such as the Western Pampas (Winter, 1999; Ferone and Devito, 2004), we argue that their importance changed during years of extended flooding when a connectivity threshold is crossed. We found that the number of water bodies declined dramatically between 2000 and 2001, even though the surface water coverage increased (Figure 3a). Whereas, the average water body size decreased in this year as new small water bodies appeared, the regional surface water coverage was mainly attributed to large-sized water bodies. It is in this situation where surface lateral movements may gain importance. When a more detailed analysis was performed, we found that in lowlands, the ten largest water bodies represented more than 75% of the surface water coverage in 2001, whereas, they only represented 38% in 2000 (Figure 7). The function of cumulative surface water coverage versus water body size (from largest to smallest) revealed a more abrupt slope at the flood peak in 2001, showing an increasing importance of large-sized water bodies. Interestingly, these functions crossed-over between the previous (2000) and posterior (2002) years to the flood peak (Figure 7) suggesting that although total flooded area retracted to lower levels in 2002 than in 2000, water bodies remained larger, or in other words, took longer to retract than smaller ones. This is expected to cause profound changes in the distribution and continuity of the area covered by free water in the landscape. For instance, the development of the biggest water body in 2001 connected distant areas as far as 75 km away in the NE–SW bearing. This dynamics can explain the fact that, regionally, poorly synchronized rainfall yielded increasingly synchronized patterns of water-table level and surface water coverage variation with a large scale flood being the emergent result. Remarkably, local settlers and workers have reported events of massive laminar water displacement, often precipitated by water bodies overcoming linear topographic barriers such as roads or railways during spring of 2001 (local newspapers and contingency reports).

Estimates of seasonal mass variation provided by GRACE proved to be a useful proxy of water storage. Several studies have compared the changes in water storage derived from GRACE gravity measurements with in situ data of soil moisture and groundwater level, or with estimates based on water balance computations, streamflow, and altimetry of large water bodies (Strassberg *et al.*, 2007; Yirdaw *et al.*, 2008; Strassberg *et al.*, 2009; Swenson and Wahr, 2009). Most of these studies were carried out in arid or semiarid regions, with deep groundwater, and were performed at the catchment scale. In this study, we found that GRACE estimates performed relatively well in a sub-humid area where groundwater and surface water are closely linked. The

changes described by GRACE were consistently higher than those suggested by groundwater and surface water measurements. The difference can be attributed to the unsaturated soil water component that was not taken into account in our estimations. This component could potentially account for a thickness of ±300 mm if we assume a regional average unsaturated soil thickness of 2 m (depth from the surface to the water table) and a 15% volumetric water storage between field capacity and wilting point water potentials. Therefore, in this case, GRACE estimates can be considered a more comprehensive description of regional water storage changes and at the same time a methodological shortcut.

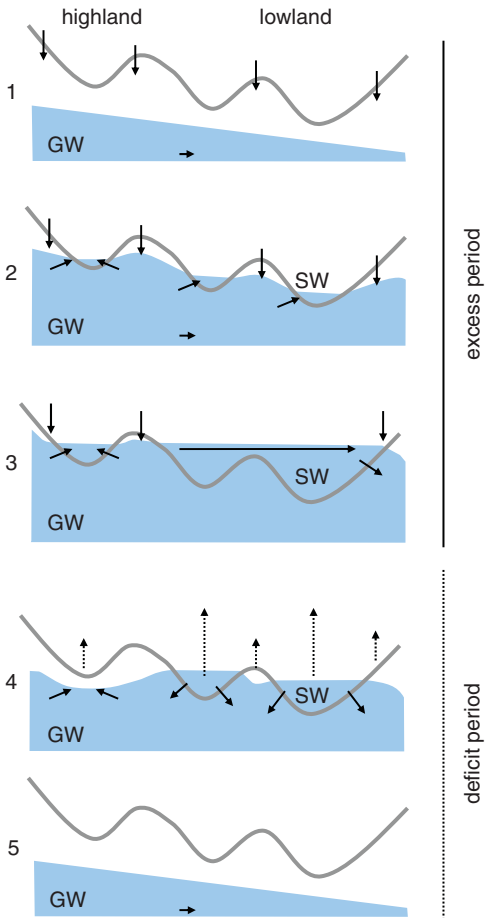

Figure 6. Schematic description of major water fluxes during a flood cycle in the Western Pampas. The initiation of a high rainfall period generates excess water (1) and the onset of water table level raises (2). At this stage GW to SW fluxes predominate in both highland and lowland sections. As the high rainfall period continues, surface water bodies grow and coalesce, favouring long distance water transport and transfer of water excesses from highland to lowland (3). At this stage, exchange between surface and groundwater becomes inverted in the lowland as a result of surface water imports and level raises. Once the high rainfall period is over and water deficit condition return, net evaporative discharge from water bodies (tank evaporation) and groundwater (phreatic water transpiration by plants) restore water levels (4). Although tank evaporation is higher than evapotranspiration in the land, suggesting the predominance of groundwater to surface water fluxes during dry periods, the large water gains of lowland surface water bodies during the wet period could sustain a net SW to GW flux for some time (4). After a few years of water deficit, groundwater levels return to the initial stage, inhibiting further evaporative groundwater discharge (5).

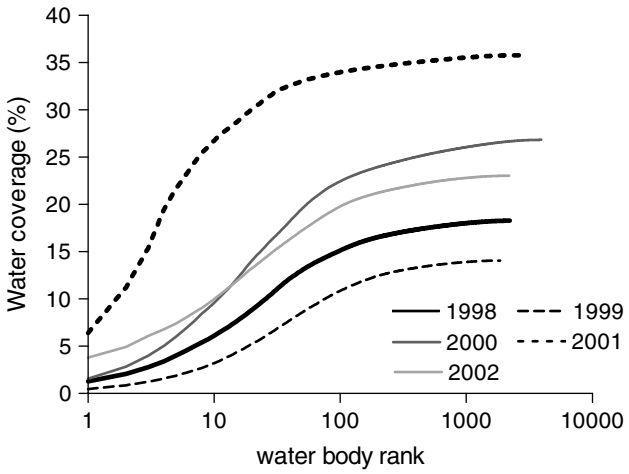

Figure 7. Relationship between the number and coverage of water bodies in the lowland section of our study region through the flooding cycle. Accumulated surface water coverage is calculated as all the individual water bodies of the study scene, from largest to smallest, are progressively taken into account. Each line corresponds to a single LANDSAT scene captured within the months of October and November of each year.

Implications for flood monitoring and management

In this study, we found that in 2001, one-fourth of the study region, that is one of the most productive areas of Argentina, was covered with water bodies. This situation undoubtedly opens challenges and conflicts to farmers and land, water, and wildlife managers trying to balance the benefits of intermediate GW depths that maximize crop yields (Nosetto *et al.*, 2009) versus shallow GW depths that cause waterlogging to crops and damage to infrastructure (Lavado and Taboada, 1988; Viglizzo and Frank, 2006) but likely play a role sustaining vast and diverse wetland ecosystems of the region (Galat *et al.*, 1998; Caziani *et al.*, 2001; Pringle, 2001; Chaneton, 2006). The fact that flooding cycles develop gradually until critical connectivity thresholds are achieved opens the possibility for the development of an early warning system of value to public and private stake-holders involved in land management.

It is important to consider that when climate emerges as a major driver of flooding cycles, its interaction with land cover and land use decisions can be similarly important in shaping the hydrology of the flattest portions of the Pampas (Nosetto *et al.*, 2008, 2009; Viglizzo *et al.*, 2009). Hence, an appropriate monitoring system should specifically incorporate groundwater and surface water information, in addition to rainfall data, and include the characterization of water body coalescence or size changes. Importantly, many remote sensing tools are nowadays available to public use and can substantially facilitate the design and implementation of an early warning alarm system. In this study, we evaluated and incorporated: (i) TRMM precipitation data provided by TOVAS (Kummerow *et al.*, 1998), which showed a good correlation with ground measurements, (ii) radiometric (LANDSAT) and interferometric (ENVISAT), which probed useful to characterize the area and level of surface water

bodies, respectively, and (iii) GRACE data that successfully described water storage shifts (Rodell and Famiglietti, 2002). In addition to these useful remote sensing tools, a monitoring system would benefit from a more extended, up to date phreatimetric network, that is currently in progress for this area (Nosetto *et al*., 2009). An alarm system that assimilates these sources of information, as opposed to one that is solely based on climatic data, would improve our understanding, prediction, and adaptative management of floods under the fast land use change conditions of the Pampas.

ACKNOWLEDGEMENTS

This work was by grants from the Inter-American Institute for Global Change Research (IAI, CRN II 2031), which is supported by the US National Science Foundation (Grant GEO-0452325) and the International Development Research Center (IDRC—Canada). We thank Jean—Francois Cretaux and Martin Saraceno for ENVISAT data, Comisión Nacional de Actividades Espaciales (CONAE), Argentina for LANDSAT imagines, and Servicio Meteorológico Nacional (SMN), INTA, R. Aradas, Cámara de Cereales and private land owners for providing phreatic data. G. Baldi and M. Nosetto made valuable suggestions about the analyses and critical comments on the manuscript.

REFERENCES

Allen RG, Pereira LS, Raes D, Smith MD. 1998. *Crop Evapotranspiration. Guidelines for Computing Crop Water Requirements*. FAO: Rome; p. 328.

Alley MW, Healy RW, LaBaugh JW, Reilly TE. 2002. Flow and storage in groundwater systems. *Science* **296**: 1985–1990.

Aradas RD, Lloyd J, Wicks J, Palmer J. 2002. Groundwater problems in low elevation regional plains: The Buenos Aires Province example. In *Groundwater and Human Development*, Bocanegra E, Martinez D, Massone H (eds). Taylor & Francis: London; 613–623.

Baldi G, Paruelo JM. 2008. Land use and land cover dynamics in South American temperate grasslands. *Ecology and Society* **13**(2): 6.

Barros V, Menendez A, Nagy G. 2006. *El cambio climático en el Rıo de la Plata*. Centro de Investigaciones del Mar y la Atmósfera (CIMA): Libros del Zorzal, Buenos Aires, Argentina; 174 p.

Birkett CM, Mertes LAK, Dunne T, Costa MH, Jasinski MJ. 2002. Surface water dynamics in the Amazon Basin: application of satellite radar altimetry. *Journal of Geophysical Research* **107**: DOI: 8010.1029/2001JD000609.

Brunke M, Gonser T. 1997. The ecological significance of exchange processes between rivers and groundwater. *Freshwater Biology* **37**(1): 1–33.

Caziani SM, Derlindati EJ, Talamo A, Sureda AL, Trucco CE, Nicolossi G. 2001. Waterbird Richness in Altiplano Wetlands of Northwestern Argentina. *Waterbirds: The International Journal of Waterbird Biology* **24**(1): 103–117.

Chaneton EJ. 2006. Impacto ecológico de las perturbaciones naturales. Las inundaciones en pastizales pampeanos. *Ciencia Hoy* **16**: 18–32.

De Löe R. 2008. Floodplain management in Canada: overview and prospects. *Canadian Geographer* **44**(4): 355–368.

Dıaz-Zorita M, Pepi M, Grosso G. 1998. *Estudio de las precipitaciones en el oeste bonaerense*. EEA INTA: Buenos Aires, INTA, Villegas, Argentina; 15 p.

Dingman LS. 1993. *Physical Hydrology*. Prentice Hall: New Jersey; 575 pp.

Ferone JM, Devito KJ. 2004. Shallow groundwater-surface water interactions in pond-peatland complexes along a Boreal Plains topographic gradient. *Journal of Hydrology* **292**: 75–95.

Frappart F, Calmant S, Cauhope M, Seyler F, Cazenave A. 2006. Preliminary results of ENVISAT RA-2-derived water levels validation over the Amazon basin. *Remote Sensing of Environment* **100**: 252–264.

Friedl MA, Brodley CE. 1997. Decision tree classification of land cover from remotely sensed data. *Remote Sensing of Environment* **61**: 399–409.

Fuschini Mejía MC. 1994. *El agua en las llanuras*. UNESCO/ORCYT: Montevideo, Uruguay; 59 pp.

Galat DL, Fredrickson LH, Humburg DD, Bataille KJ, Bodie JR, Dohrenwend J, Gelwicks GT, Havel JE, Helmers DL, Hooker JB, Jones JR, Knowlton MF, Kubisiak J, Mazourek J, McColpin AC, Renken RB, Semlitsch RD. 1998. Flooding to restore connectivity of regulated, large-river wetlands. *Bioscience* **48**(9): 721–733.

Iriondo M. 1999. Climatic changes in the South American plains: records of a continent-scale oscillation. *Quaternary International* **57/58**: 93–112.

Jackson RB, Jobbágy EG, Nosetto MD. 2009. Ecohydrology bearings—invited commentary. Ecohydrology in a human-dominated landscape. *Ecohydrology* **2**: 383–389. DOI: 10.1002/eco.81nb b nv.

Jobbágy EG, Jackson RB. 2004. Groundwater use and salinization with grassland afforestation. *Global Change Biology* **10**: 1299–1312.

Jobbágy EG, Nosetto MD, Santoni CS, Baldi G. 2008. El desafío ecohidrológico de las transiciones entre sistemas leñosos y herbáceos en la llanura Chaco-Pampeana. *Ecologia Austral* **18**: 305–322.

Johnson C, Millett BV, Gilmanov T, Voldseth RA, Guntenspergen GR, Naugle DE. 2005. Vulnerability of northern prairie wetlands to climate change. *Bioscience* **55**(10): 863–872.

Kummerow C, Barnes W, Kozu T, Shiue J, Simpson J. 1998. The tropical rainfall measuaring mission (TRMM) sensor package. *Journal of Atmospheric and Oceanic Technology* **15**: 809–817.

Lavado RS, Taboada MA. 1988. Water, salt and sodium dynamics in a natraquoll in Argentina. *CATENA* **15**: 577–594.

Martin SL, Soranno PA. 2006. Lake landscape position: relationships to hydrologic connectivity and landscape features. *Limmnology and Oceanography* **51**(2): 801–814.

Nosetto MD, Jobbagy EG, Jackson RB, Sznaider GA. 2009. Reciprocal influence of crops and shallow ground water in sandy landscapes of the Inland Pampas. *Field Crop Research* **113**: 138–148. DOI: 10.1016/j.fcr.2009.04.016.

Nosetto MD, Jobbágy EG, Tóth T, Jackson RB. 2008. Regional patterns and controls of ecosystem salinization with grassland afforestation along a rainfall gradient. *Global Biogeochemical Cycles* **22**: GB2015. DOI: 10.1029/2007 GB003000.

Poole GC, Stanford JA, Frissell CA, Running SW. 2002. Three-dimensional mapping of geomorphic controls on flood-plain hydrology and connectivity from aerial photos. *Geomorphology* **48**: 329–347.

Pratharpar SA, Qureshi AS. 1998. Modelling the effects od deficit irrigation on soil salinity, depth to water table and transpiration in semid-arid zones with monsoonal rains. *International Journal of Water Resources Development* **15**: 141–159.

Pringle CM. 2001. Hydrologic connectivity and the management of biological reserves: a global perspective. *Ecological Applications* **11**(4): 981–998.

Reicosky DC, Smith RCG, Meyer WS. 1985. Foliage temperature as a means of detecting stress of cotton subjected to a short-term water-table gradient. *Agricultural and Forest Meteorology* **35**: 193–203.

Rodell M, Famiglietti JS. 2002. The potential for satellite based monitoring of groundwater storage changes using GRACE: the high plains aquifer, central US. *Journal of Hydrology* **263**(1–4): 245–246.

Schilling KE, Zhang YK, Drobney P. 2004. Water table fluctuations near an incised stream, Walnut Creek, Iowa. *Journal of Hydrology* **286**: 236–248.

Smerdon BD, Devito KJ, Mendoza CA. 2005. Interaction of groundwater and shallow lakes on outwash sediments in the sub-humid Boreal Plains of Canada. *Journal of Hydrology* **314**: 246–262.

Sophocleous M. 2002. Interactions between groundwater and surface water: the state of the science. *Hydrogeology Journal* **10**: 52–67.

Soriano A, Leon RJC, Sala OE, Lavado RS, Deregibus VA, Cahuepe M, Scaglia OA, Velazquez CA, Lemcoff JH. 1991. Rıo de la Plata Grasslands. *In Natural Grasslands: Introduction and Western Hemisphere. Ecosystems of the World*, Coupland RT (ed). Amsterdam: Elsevier; 367–407.

Strassberg G, Scanlon BR, Chambers D. 2009. Evaluation of groundwater storage monitoring with the GRACE satellite: case study of the high plains aquifer, central United States. *Water Resources Research* **45**: W05410. DOI: 10.1029/2008WR006892.

Strassberg G, Scanlon BR, Rodell M. 2007. Comparison of seasonal terrestrial water storage variations from GRACE with groundwater-level measurements from the High Plains Aquifer (USA). *Geophysical Research Letters* **34**: L14402. DOI:10.1029/2007GL030139.

Su F, Hong Y, Lettenmaier DP. 2008. Evaluation of TRMM multisatellite precipitation analysis (TMPA) and its utility in hydrologic prediction in the La Plata Basin. *Journal of Hydrometeorology* **9**: 622–640.

Swenson S, Wahr J. 2009. Monitoring the water balance of Lake Victoria, East Africa, from space. *Journal of Hydrology* **379**: 163–176.

Swenson S, Wahr J, Milly PCD. 2003. Estimated accuracies of regional water storasge variations inferred from gravity recovery and climate experiment (GRACE). *Water Resource Research* **39**(8): 1223.

Tapley BD, Bettadpur S, Ries JC, Thompson PF, Watkins MM. 2003. GRACE measurements of mass variability in the Earth System. *Science* **23**(5683): 503–505.

Toth J. 1999. Groundwater as a geologic agent: an overview of the causes, processes, and manifestations. *Hydrogeology Journal* **7**(1): 1–14.

Viglizzo EF, Frank FC. 2006. Ecological interactions, feedbacks, thresholds and collapses in the Argentine Pampas in response to climate and farming during the last century. *Quaternaly International* **158**(1): 122–126.

Viglizzo EF, Jobbagy EG, Carreño LV, Frank FC, Aragón R, Oro LD, Salvador VS. 2009. The dynamics of cultivation and floods in arable lands of central Argentina. *Hydrology and Earth System Sciences* **13**: 491–502.

Viglizzo EF, Roberto ZE, L'ertora FA, Gay EL, Bernardos J. 1997. Climate and land-use change in field crop ecosystems of Argentina. *Agricultural, Ecosystems and Environment* **66**: 61–70.

Ward JV, Malard F, Tockner K. 2002. Landscape ecology: a framework for integrating pattern and process in river corridors. *Landscape Ecology* **17**(Supplement 1): 35–45.

Winter T. 1999. Relation of streams, lakes, and wetlands to groundwater flow systems. *Hydrogeology Journal* **7**: 28–45.

Yirdaw SZ, Snelgrove KR, Agboma CO. 2008. GRACE satellite observations of terrestrial moisture changes for drought characterization in the Canadian Prairie. *Journal of Hydrology* **356**: 84–92.

